Validation of polymorphic Gompertzian model of cancer through in vitro and in vivo data

Soboleva, A.; Kaznatcheev, Artem; Cavill, Rachel; Schneider, Katharina; Staňková, K.

DOI
10.1371/journal.pone.0310844

Publication date
2025

Document Version
Final published version

Published in
PLoS ONE

PLOS ONE

RESEARCH ARTICLE

Validation of polymorphic Gompertzian model of cancer through *in vitro* and *in vivo* data

Arina Soboleva[1]*, **Artem Kaznatcheev**[2], **Rachel Cavill**[3], **Katharina Schneider**[3], **Kateřina Staňková**[1]

1 Institute for Health Systems Science, Faculty of Technology, Policy and Management, Delft University of Technology, Delft, The Netherlands, **2** Department of Mathematics and Department of Information and Computing Sciences, Utrecht University, Utrecht, The Netherlands, **3** Department of Advanced Computing Sciences, Faculty of Science and Engineering, Maastricht University, Maastricht, The Netherlands

* a.soboleva@tudelft.nl

Citation: Soboleva A, Kaznatcheev A, Cavill R, Schneider K, Staňková K (2025) Validation of polymorphic Gompertzian model of cancer through *in vitro* and *in vivo* data. PLoS ONE 20(1): e0310844. https://doi.org/10.1371/journal.pone.0310844

Editor: Julio Cesar de Souza, Universidade Federal de Mato Grosso do Sul, BRAZIL

Received: September 18, 2023

Accepted: September 6, 2024

Published: January 9, 2025

Data Availability Statement: The in vitro data is available in Artem Kaznatcheev's GitHub at https://github.com/kaznatcheev/GameAssay. The in vivo data is published as supplementary of Ghafari Laleh's et al. paper (https://doi.org/10.1371/journal.pcbi.1009822.s006).

Funding: This research was funded by H2020 Marie Sklodowska-Curie Actions (https://marie-sklodowska-curie-actions.ec.europa.eu/) (Award number 955708 [KS]) and Nederlandse Organisatie voor Wetenschappelijk Onderzoek (https://www.

Abstract

Mathematical modeling plays an important role in our understanding and targeting therapy resistance mechanisms in cancer. The polymorphic Gompertzian model, analyzed theoretically and numerically by Viossat and Noble to demonstrate the benefits of adaptive therapy in metastatic cancer, describes a heterogeneous cancer population consisting of therapy-sensitive and therapy-resistant cells. In this study, we demonstrate that the polymorphic Gompertzian model successfully captures trends in both *in vitro* and *in vivo* data on non-small cell lung cancer (NSCLC) dynamics under treatment. Additionally, for the *in vivo* data of tumor dynamics in patients undergoing treatment, we compare the goodness of fit of the polymorphic Gompertzian model to that of the classical oncologic models, which were previously identified as the models that fit this data best. We show that the polymorphic Gompertzian model can successfully capture the U-shape trend in tumor size during cancer relapse, which can not be fitted with the classical oncologic models. In general, the polymorphic Gompertzian model corresponds well to both *in vitro* and *in vivo* real-world data, suggesting it as a candidate for improving the efficacy of cancer therapy, for example, through evolutionary/adaptive therapies.

Introduction

For patients with advanced cancer, an aggressive treatment aiming at complete cancer eradication is often ineffective [1–3]. Instead of pursuing tumor elimination through maximum tolerable dose (MTD), novel therapies, called evolutionary or adaptive therapies, aim to anticipate and steer cancer eco–evolutionary dynamics to maximize patients' quality and quantity of life [3–18]. Mathematical models of cancer's response to therapy may help us to improve therapies and, perhaps even more importantly, are needed to understand conditions under which the evolutionary therapies outperform standard of care [5, 15, 19–30].

nwo.nl/) (Award numbers VI.Vidi.213.139 and OCENW.KLEIN.277 [KS]). The funders had no role in study design, data collection and analysis, decision to publish, or preparation of the manuscript.

Competing interests: The authors have declared that no competing interests exist.

Recently, Viossat and Noble analyzed a group of density-dependent polymorphic models with two types of cancer cells, therapy-resistant and therapy-sensitive ones, and demonstrated that the containment protocol, which aims to keep the tumor burden below a particular threshold for as long as possible, outperforms standard treatment in all these models in terms of time to progression [31]. Their numerical simulations demonstrating this result were performed on one of these models, a two-population Gompertzian model. The model assumes equal growth rates for the sensitive and resistant populations, density-dependent selection, and no cost of resistance, i.e., no assumption that the resistant cells are less fit than the sensitive ones when therapy is not applied [14, 25, 32, 33]. The model assumes no direct competition between different cell types through competition coefficients but a shared carrying capacity instead. The absence of the cost of resistance makes the model applicable to a broader range of cancer types, as it was suggested that in some cancers, resistance does not need to have a cost [5, 32, 34, 35].

Before bringing the polymorphic Gompertzian model to clinical practice, its ability to fit the real-world data should be evaluated [36, 37]. In this study, we therefore test the polymorphic Gompertzian model's agreement with *in vitro* data from Kaznatcheev et al. [34] and *in vivo* data from previous clinical studies [38–42] of non-small cell lung cancer (NSCLC) dynamics under therapy.

Materials and methods

The polymorphic Gompertzian model of cancer analyzed by Viossat and Noble assumes two types of cancer cell populations—sensitive and resistant to treatment—with sizes $S(t)$ and $R(t)$ at time t, respectively [31]. The total size of cancer population at time t is $N(t) = S(t) + R(t)$. The dynamics of the two populations are described by the ordinary differential equations:

$$\dot{S}(t) = \rho \ln\left(\frac{K}{N(t)}\right)(1 - \lambda C(t))S(t), \tag{1}$$

$$\dot{R}(t) = \rho \ln\left(\frac{K}{N(t)}\right)R(t), \tag{2}$$

where $C(t)$ is treatment dosage at time t, K is carrying capacity of the tumor (that defines the maximum possible size to which the cancer population can grow), ρ is growth rate of cancer cells, and λ is treatment sensitivity.

Note that competition between sensitive and resistant cells is not explicitly present in the model, besides competing for space and resources through the carrying capacity. The model also assumes the same growth rate ρ for both populations and no cost of resistance.

Fitting the model to *in vitro* data

We first validated the polymorphic Gompertzian model on *in vitro* data from the study by Kaznatcheev et al. [34]. In their study, two populations of NSCLC cells—sensitive and resistant to treatment—were seeded at different initial proportions with and without addition of cancer-associated fibroblasts (CAF) and the immunotherapy drug Alectinib. In total, the data contains 192 wells: eight different seeding proportions of sensitive cells (0, 0.1, 0.2, 0.4, 0.6, 0.8, 0.9, 1) in four conditions: with and without drug and with and without CAF, and six replicates for each combination. For all wells, sizes of sensitive and resistant populations over time are presented.

We fitted the population dynamics of sensitive and resistant cells for each of the 192 wells to the polymorphic Gompertzian model using the Python GEKKO package [43], with mean

squared error (*MSE*) as the objective function:

$$MSE_S = \frac{1}{n}\sum_{i=1}^{n}(S_{pred}(t_i) - S_{mes}(t_i))^2, \tag{3}$$

$$MSE_R = \frac{1}{n}\sum_{i=1}^{n}(R_{pred}(t_i) - R_{mes}(t_i))^2, \tag{4}$$

where $S_{mes}(t_i)$ and $R_{mes}(t_i)$ are measured sizes of sensitive and resistant populations at i-th time point, respectively, and $S_{pred}(t_i)$ and $R_{pred}(t_i)$ are model-predicted sensitive and resistant population sizes at i-th time point, respectively. Parameter n determines the number of time points.

In the fitting procedure, we exploited the explicit treatment modeling through variable $C(t_i)$, the treatment dosage at time t_i. In wells where the drug was not applied, we set $C(t_i) = 0$ for all t_i. The dynamics in wells with drug were modeled as the treatment variable $C(t_i)$ set to 0 in time points $t_i < 20$ hours and to 1 at time points $t_i \geq 20$ hours. This way, we reflected the conditions of the original experiment, where Alectinib was added to the wells 20 hours after seeding [34]. As CAF have a variety of functions and action mechanisms [44], which are challenging for direct modeling, we evaluated their effect implicitly through a comparison of the fitted model's parameter values (K, ρ, λ) in wells with and without CAF. In wells with seeding proportions 0 and 1 (fully resistant and sensitive wells), we set the measurements of the minor population to zero before fitting the model, as their nonzero measurements present only fluorescent noise. After the polymorphic Gompertzian model was fitted to the measurements, the obtained parameter values and their dependence on the initial proportions of sensitive cells and experimental conditions were analyzed.

Fitting the model to *in vivo* data

In vivo data come from clinical trials of patients with non-small cell lung cancer (NSCLC) who were treated with either the immunotherapy drug Atezolizumab or the chemotherapy drug Docetaxel [38–42]. We used a fully anonymized subset of the data, published by Ghaffari Laleh's et al. [38], to ensure reproducibility. The implemented dataset contains only time-series data of the target lesion volumes that were estimated following the common assumption that the tumor is a sphere with a diameter equal to the longest measured lesion diameter [45].

Focusing on the tumors with six or more measurements over time, we split the resultant 587 patient cases into five categories based on the trend in the measured data: "Growth", "Decline", "Delayed response", "U-shape" or "Fluctuate" (For details, see S2 Appendix). We fitted the polymorphic Gompertzian model to the tumor volumes of each of the 587 patients using the Python package GEKKO [43]. We fit the model parameters so that the *MSE* between measured data and the sum of model-predicted sensitive and resistant population sizes defined as

$$MSE = \frac{1}{n}\sum_{i=1}^{n}\Big((R_{pred}(t_i) + S_{pred}(t_i)) - x_{mes}(t_i)\Big)^2 \tag{5}$$

is minimized. In (5), $x_{mes}(t_i)$ is measured tumor volume at time t_i, $R_{pred}(t_i)$ and $S_{pred}(t_i)$ are model-predicted resistant and sensitive population volumes at time t_i, respectively, and n is number of time points.

As the *in vivo* data contains only total population sizes, initial proportions of sensitive cells were estimated through a grid search (S1 Appendix). We modeled the treatment as a constant function $C(t_i) = 1$, as in the clinical studies patients received chemotherapy or immunotherapy

regularly and at the same dose [39–42]. After obtaining the best fitting parameters, we analyzed the accuracy of the fit in different trend categories (S4 Appendix). We also fitted two best performing classical models of Laleh's et al.'s study [38]—General Gompertz and General von Bertalanffy models—to the *in vivo* data and compared accuracy of the three models within the trend categories (See S3 Appendix for more details on the fitting of the classical models and the assessment of the models' accuracy).

Results

Validation through *in vitro* data

The fit of the polymorphic Gompertzian model to Kaznatcheev et al.'s data. We fitted the polymorphic Gompertzian model to *in vitro* dynamics of sensitive and resistant cancer populations. The model's fit to the measured data in four experimental conditions (Drug-, CAF-; Drug-, CAF+; Drug+, CAF-; Drug+, CAF+) and with seeding proportions of sensitive cells is presented in Fig 1. Columns represent the experimental conditions of wells. Each row contains wells from one of the intended proportion groups (0.2, Â 0.4, Â 0.6, Â 0.8)

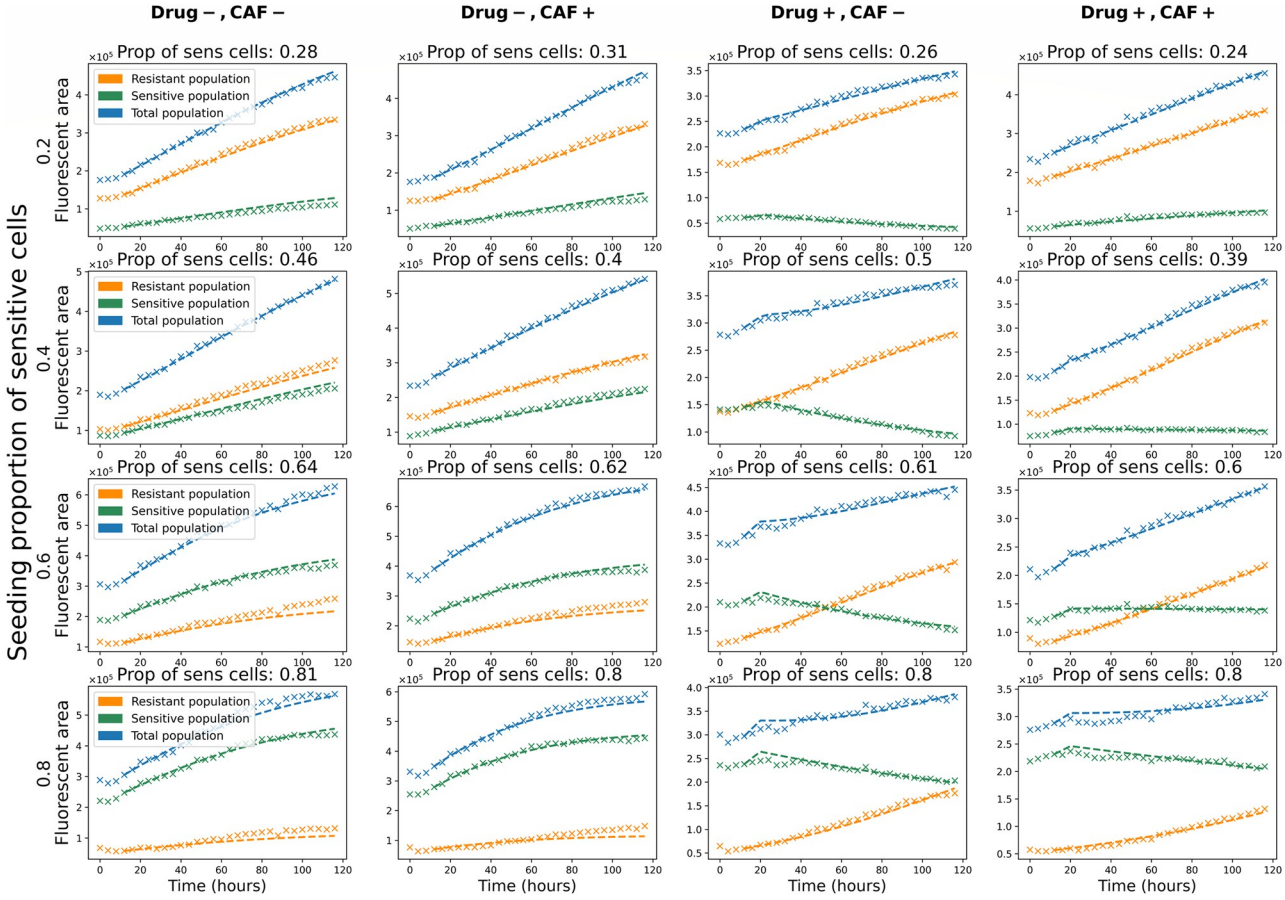

Fig 1. The polymorphic Gompertzian model's fit to *in vitro* data. Fit of the polymorphic Gompertzian model to *in vitro* dynamics of sensitive, resistant and total cancer cell populations across four experimental conditions and different initial ratios of sensitive cells. Each graph displays the measured cell counts (crosses) and the model fit (lines) to one well. Sensitive, resistant, and total populations are colored in green, orange, and blue, respectively. For each well measured proportion of sensitive cells at time point $t_3 = 12h$ (start of the model's fit) is stated above the graph. Columns represent experimental conditions (presence or absence of drug and CAF). Rows contain wells in different conditions with similar initial proportions of sensitive cells.

https://doi.org/10.1371/journal.pone.0310844.g001

corresponding to the seeding proportions of sensitive cells. The actual proportions in wells differ from the intended ones due to experimental variations.

The trend dynamics were captured well for all experimental and initial conditions. In particular, the model reflected the convex form of the population growth with a slowing of the growth rate closer to a larger size (rows 3 and 4 of Fig 1). We modeled the therapy start at $t_i = 20h$ following the experimental setting and, thus, were able to capture the change of the trend in the sensitive population (columns 3 and 4 of Fig 1). The population is initially growing, but starts to decline once the treatment is added. In the wells with the drug applied (columns 3 and 4 of Fig 1) the model is able to simultaneously capture the decline of the sensitive population and the growth of the resistant population.

In the wells where the sizes of the sensitive and the resistant populations differ significantly, the model fitted the dynamics of the larger population better than the smaller population. This effect is attributed to the common growth rate ρ and carrying capacity K shared by the sensitive and resistant cancer populations (Eqs (1) and (2)). The optimization led to a higher weight to the dynamics of a larger population, to decrease the total fitting error. While the relative error of the smaller population increased with the decrease of its proportion, the error for the total population stayed below 5% mean absolute percentage error (*MAPE*) for all proportions (Fig 2). In monotypic wells (seeding proportions of sensitive cells equal 0 or 1) the error of the model's fit to the non-seeded population is zero.

Fig 2 also shows that in wells with treatment (Drug+, CAF- and Drug+, CAF+), model accuracy was generally higher than in those without drug. This can be explained by the higher number of parameters in cases with a drug (treatment sensitivity λ was fitted only if treatment was present).

Fig 3 shows model parameters over wells with different initial ratios of sensitive cells and experimental conditions (presence or absence of drug and CAF). The treatment sensitivity parameter λ is significantly smaller in wells where CAF are present, which was confirmed using a Welch's unequal variance t-test (p-value = 10^{-7}). The test repeated with exclusion of the outliers ($S = 0$ or $R = 0$) confirmed the result. Since λ represents the magnitude of drug effect on sensitive cells, smaller values of λ reflect reduced efficiency of the treatment when CAFs are present.

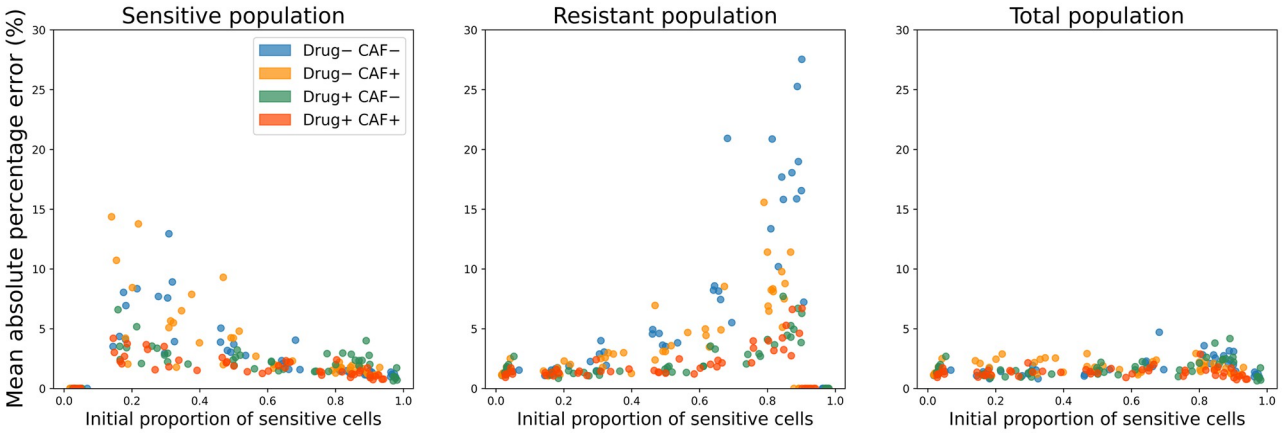

Fig 2. Mean Absolute Percentage Error (MAPE) of the polymorphic Gompertzian model's fit to *in vitro* data. MAPEs of the model's fit to dynamics of sensitive, resistant and total cancer cell populations are presented for a range of initial proportion of sensitive cells. Data points are colored according to experimental conditions of the well (presence or absence of drug and CAF).

https://doi.org/10.1371/journal.pone.0310844.g002

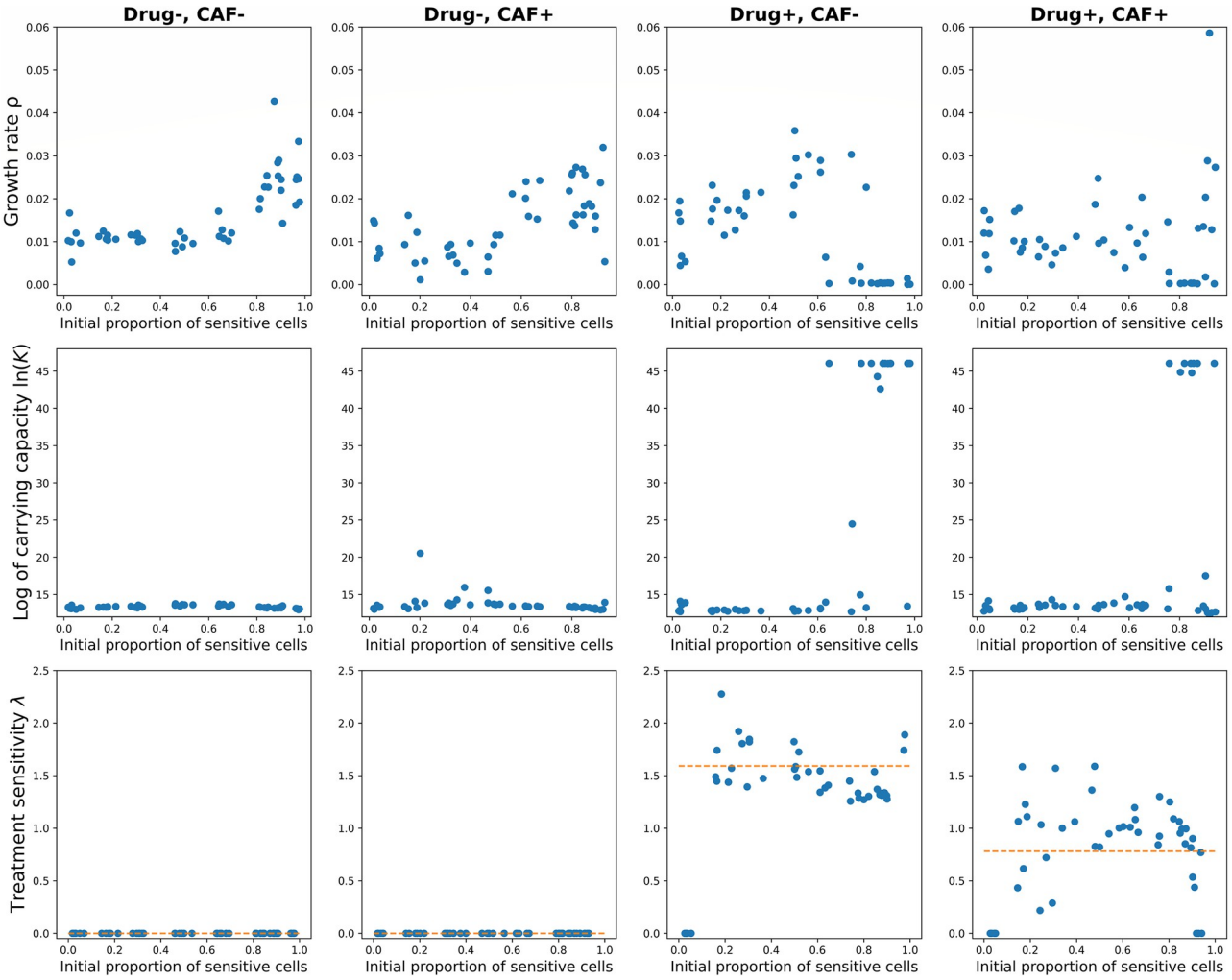

Fig 3. Distribution of the polymorphic Gompertzian model's parameters across *in vitro* wells. Parameters of the polymorphic Gompertzian model fitted to *in vitro* data across four experimental conditions (indicated in columns) and range of initial proportions of sensitive cells. Each dot in the graphs corresponds to the parameter value of the model fitted to dynamics from one well. The orange line indicates the mean value of treatment sensitivity λ in a given experimental condition.

https://doi.org/10.1371/journal.pone.0310844.g003

Effect of cancer-associated fibroblasts on the model fit. In Fig 3 we also observe a sudden increase in the fitted carrying capacity K and related decay in the fitted growth rate ρ for several wells with $p \geq 0.6$ and drug present. In these cases, a very high K value makes the term $\ln\left(\frac{K}{N}\right)$ almost constant for the entire measured period (changes in N have nearly no effect, as $K \gg N(t), \forall t$). At the same time, a low growth rate ρ compensates for the magnitude of $\ln\left(\frac{K}{N}\right)$. Such parameter values result in an exponential growth for resistant population and an exponential decrease for sensitive population, reflecting the trends observed in the data. We can conclude that for the cases with prevailing sensitive population and drug applied the dynamics switches from Gompertzian to exponential growth/decay (See S5 Appendix for more details).

Validation through *in vivo* data

The model's fit to different trend categories. We divided the *in vivo* data into groups based on the displayed trend in tumor growth and evaluated the model's performance in each

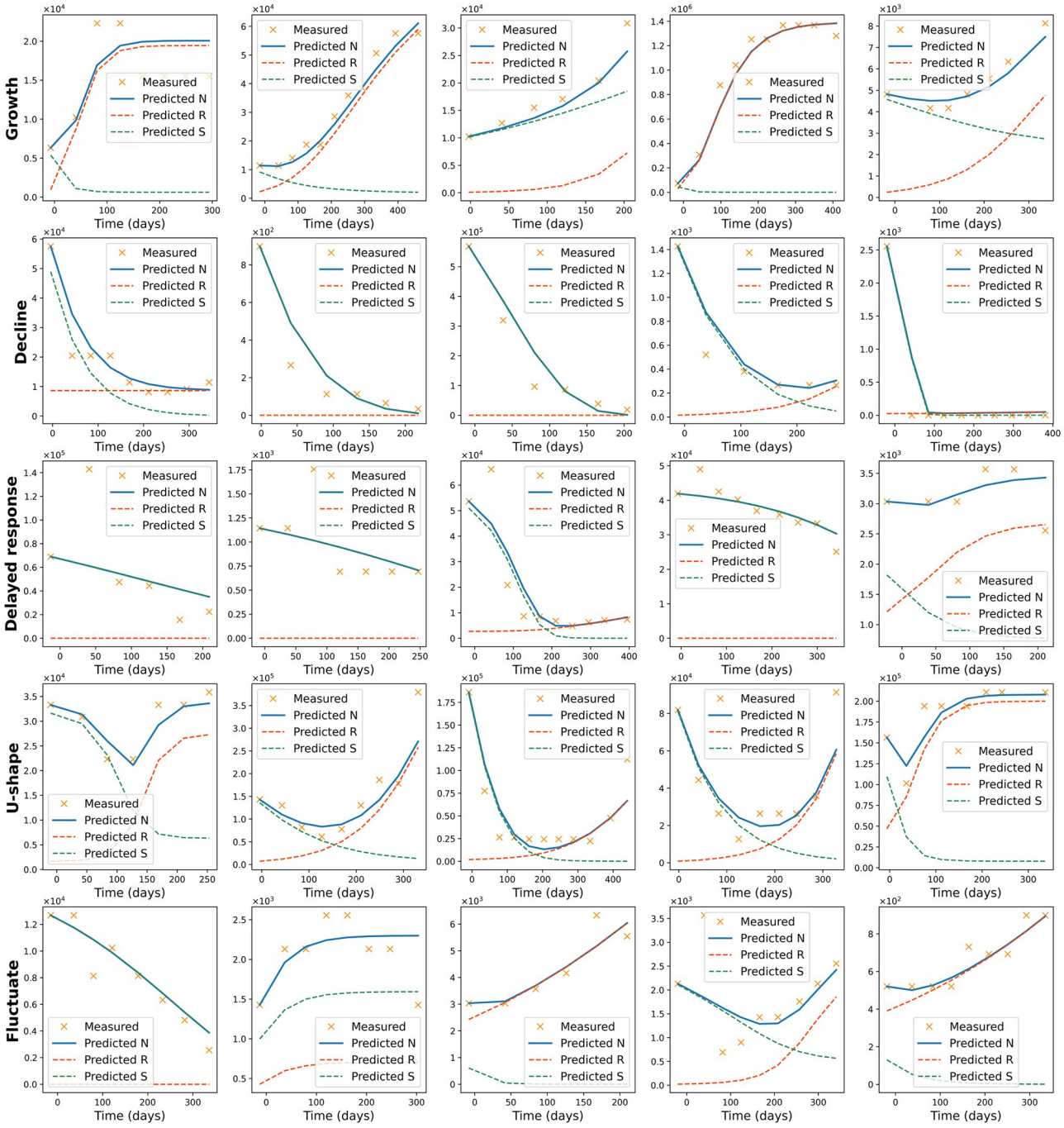

Fig 4. The fit of the polymorphic Gompertzian model to *in vivo* data across five trend categories. Each row shows five patient cases corresponding to one of the trend categories: "Growth", "Decline", "Delayed response", "U-shape" or "Fluctuate". Measured tumor volume over time is marked with orange crosses. The blue line represents the model's fit to the total tumor size dynamics, green and orange lines represent predicted dynamics of sensitive and resistant populations sizes respectively.

https://doi.org/10.1371/journal.pone.0310844.g004

of these categories. Fig 4 presents the polymorphic Gompertzian model's fit to five representative patient cases from each trend category. The two top rows show that the model can accurately capture both "Growth" and "Decline" trends. In these categories, one of the populations has a significantly larger effect on the total population dynamics. In the "Growth" category, the

Table 1. Comparison of the models' fit errors in trend categories. The table presents *p*-values of *t*-tests between two groups of nMSE. Bold text indicates statistically significant *p*-values.

		Poly Gomp	Gen Gomp	Gen Bert
Growth	Poly Gomp	1		
	Gen Gomp	**0.007**	1	
	Gen Bert	0.1	**0.001**	1
Decline	Poly Gomp	1		
	Gen Gomp	$\mathbf{2 \cdot 10^{-6}}$	1	
	Gen Bert	0.5	$\mathbf{2 \cdot 10^{-6}}$	1
Del Resp	Poly Gomp	1		
	Gen Gomp	0.2	1	
	Gen Bert	0.4	**0.04**	1
U-shape	Poly Gomp	1		
	Gen Gomp	$\mathbf{9 \cdot 10^{-8}}$	1	
	Gen Bert	$\mathbf{7 \cdot 10^{-7}}$	0.4	1
Fluctuate	Poly Gomp	1		
	Gen Gomp	**0.02**	1	
	Gen Bert	1	**0.01**	1

https://doi.org/10.1371/journal.pone.0310844.t001

increase of the tumor size is attributed to the proliferation of the resistant population. In the "Decline" category, in contrast, the sensitive population plays a major role, forming the downward trend of the total population size. The polymorphic Gompertzian model is also successful in describing the "U-shape" trend in the data due to incorporated heterogeneity. In this case, sensitive population initially prevails but then decreases under treatment. As the result, resistant population is able to proliferate without competition for space and resources, which leads to regrowth of the tumor.

The model is unable to capture the "Delayed response" trend. The model tends to ignore initial tumor size increase and fits the data as a monotonic decline. In some cases, where the response is delayed longer, the model describes it as a growth trend and does not capture the subsequent decline (5th graph in the "Delayed response" row of Fig 4). In the "Fluctuate" category, the polymorphic Gompertzian model estimates data dynamics with a monotonic growth, a monotonic decline, or a U-shape trend. The model is often able to capture the main tendency in the data but ignores smaller fluctuations.

Overall, the lowest mean errors of the model's fit correspond to "Growth" and "Decline" categories and the highest mean error corresponds to the "Delayed response" trends (S4 Appendix). We also conclude that the polymorphic Gompertzian model presents a higher accuracy in the majority of cases, compared to the monomorphic Gompertz and General van Bertalanffy models. The normalized *MSE* of the models' fits were compared in the trend categories. Table 1 presents *p*-values of the *t*-test. The mean error of the polymorphic Gompertzian model's fit is smaller than that of the General Gompertz model in the "Growth" and "Decline" categories and similar to that of the General von Bertalanffy model. None of the models is capable of describing the "Delayed response" trend and the error values in this category are similar for all three models. The polymorphic Gompertzian model demonstrates a higher accuracy than the other models in the "U-shape" category (See S3 Appendix for details).

Discussion

We validated the polymorphic Gompertzian model of Viossat and Noble [31] using *in vitro* and *in vivo* data. Overall, the model fits both studied cases very well. The model assumes (i) a

shared carrying capacity between sensitive and resistant cell populations, (ii) the growth rate of the two populations being equal in the absence of drug, and (iii) no competition/cooperation effects in terms of a competition/fitness matrix. Due to these assumptions, we were not able to re-evaluate all conclusions of Kazatcheev et al's game-theoretic model [34].

The polymorphic Gompertzian model may be perceived as implicitly frequency-dependent in the *in vitro* case, as the growth of the sensitive and resistant populations is dependent on the seeding proportions and as we fitted the model's parameters separately for different initial proportions of sensitive cells. Nevertheless, the model's assumptions allowed it to fit both the rich data from *in vitro* experiments and the sparse data from *in vivo* clinical studies.

With the polymorphic Gompertzian model, we took a conceptually different approach to the analysis of the Kaznatcheev et al. [34] *in vitro* data. Kaznatcheev et al. [34] specifically designed a new experimental procedure as a way to measure a competition/fitness matrix [46] that allowed for two distinct fitness functions for the sensitive and resistant cell types, but ignored population dynamics which we considered very important in this work. We showed that the polymorphic Gompertzian model could accurately capture the trends in the data with a growth rate ρ that is the same for the sensitive and resistant types. We confirmed the anti-treatment effect of cancer-associated fibroblasts. However, we could not confirm or reject Kaznatcheev's et al. [34] conclusion on strong violations of the cost of resistance (where resistant cells are fitter than sensitive cells even without treatment). Therefore, we believe that a more structural approach needs to be adopted to fit the data, to avoid conclusions implied by the model assumptions rather than by the real cancer cells' growth.

The future work shall consider extensions of the polymorphic Gompertzian model to cases where sensitive and resistant cells are allowed to have different growth rates and/or when frequency-dependent selection is included in the form of a competition matrix. Such extensions can be tested on other existing or proposed *in vitro* datasets that provide data on different cell type proportions [47–50] or population sizes [38, 51, 52].

In this study, we demonstrated that the polymorphic Gompertzian model can also be parametrized with the more sparse data from *in vivo* tumor size dynamics of patients undergoing therapy. The polymorphic Gompertzian model provides a good fit of the "Growth" and "Decline" categories, with the error comparable to the error of the best-performing classical model of cancer growth. In the "Growth" category, the polymorphic Gompertzian model described the tumor as consisting mostly of resistant cells. In the "Decline" category, if the tumor size declines monotonically to zero, then the model can treat the cancer population as completely sensitive. However, if the last few measurements show a slight increase in the tumor size, the model indicates that the resistant population is still present—allowing for the possibility of relapse and tumor regrowth. The main advantage of the polymorphic Gompertzian model is its ability to capture relapse and regrowth described clinically by the "U-shape" trend—a trend that cannot be captured by any of the six classical models analyzed by Ghaffari Laleh et al. [38].

The polymorphic Gompertzian model (along with the classic models) does not capture the "Delayed Response" trend for *in vivo* data. This could be due to the lack of information on when exactly treatment started: in clinical studies, the first measurement of the tumor size was usually performed a few days before the treatment started. Thus, the initial growth of the tumor in the "Delayed Response" trend might have happened before treatment was first applied. If we had tumor size measurements on the day the therapy started, then we could correct this. We do exactly this correction for Kaznatcheev et al. [34] *in vitro* data to capture a delayed response effect. Alternatively, the *in vivo* "Delayed Response" trend might be attributed to having insufficient concentration of the drug in the tumor at first injection. In this case, pharmacokinetics/pharmacodynamics data on drug concentration over time would be required for the polymorphic Gompertzian model to describe these cases through a time-

dependent treatment variable. Delayed differential equations may lead to a better fit of this category, too.

In our study, we demonstrated the ability of the polymorphic Gompertzian model to describe real-world data on cancer under treatment. Looking forward, the most promising future development is modeling real-world time-dependent treatment, especially adaptive therapy [15, 17, 18, 53]. The "U-shape" trend that the polymorphic Gompertzian model captures in the *in vivo* data presents an undesirable scenario for the patients. In 54 out of 81 cases in the "U-shape" category, the tumor regrows to the initial size or greater. Viossat and Noble's [31] theoretical analysis of the polymorphic Gompertzian model suggests that for these cases, the implementation of containment therapy could be beneficial and might prolong the time to tumor progression. Contradictory, Kaznatcheev et al. [34] suggest that there would be little benefit to adaptive therapy given the competition/fitness matrices that they estimated *in vitro*. Of course, in the real world, the behavior of the tumor under containment therapy may differ from the mathematical predictions and, therefore, the effectiveness of such an adaptive therapy should be thoroughly tested both theoretically and in clinical trials.

Supporting information

S1 Appendix. Procedures of fitting the polymorphic Gompertzian model to *in vitro* and *in vivo* data.
(PDF)

S2 Appendix. Trend categories in tumor volume dynamics in *in vivo* data.
(PDF)

S3 Appendix. Comparison of the polymorphic Gompertzian model's fit with the fits of the General Gompertz and General von Bertalanffy models.
(PDF)

S4 Appendix. Parameter values of the polymorphic Gompertzian model across trend categories.
(PDF)

S5 Appendix. Exponential growth and decay trends in the polymorphic Gompertzian model.
(PDF)

Author Contributions

Conceptualization: Arina Soboleva, Rachel Cavill, Katharina Schneider, Kateřina Staňková.

Data curation: Artem Kaznatcheev.

Formal analysis: Arina Soboleva.

Funding acquisition: Kateřina Staňková.

Investigation: Arina Soboleva.

Methodology: Arina Soboleva, Rachel Cavill, Katharina Schneider, Kateřina Staňková.

Software: Arina Soboleva.

Supervision: Rachel Cavill, Katharina Schneider, Kateřina Staňková.

Validation: Arina Soboleva, Artem Kaznatcheev, Kateřina Staňková.

Visualization: Arina Soboleva.

Writing – original draft: Arina Soboleva, Rachel Cavill, Katharina Schneider, Kateřina Staňková.

Writing – review & editing: Arina Soboleva, Artem Kaznatcheev, Rachel Cavill, Katharina Schneider, Kateřina Staňková.

References

1. Cronin KA, Scott S, Firth AU, Sung H, Henley SJ, Sherman RL, et al. Annual report to the nation on the status of cancer, part 1: National cancer statistics Cancer. 2022; 128(24):4251–4284. https://doi.org/10.1002/cncr.34479 PMID: 36301149
2. Jemal A, Ward EM, Johnson CJ, Cronin KA, Ma J, Ryerson AB, et al. Annual report to the nation on the status of cancer, 1975–2014, featuring survival. JNCI: Journal of the National Cancer Institute. 2017; 109(9):djx030. https://doi.org/10.1093/jnci/djx030 PMID: 28376154
3. Dujon AM, Aktipis A, Alix-Panabières C, Amend SR, Boddy AM, Brown JS, et al. Identifying key questions in the ecology and evolution of cancer. Evolutionary Applications. 2021; 14(4):877–892. https://doi.org/10.1111/eva.13190 PMID: 33897809
4. Gatenby RA. A change of strategy in the war on cancer. Nature. 2009; 459(7246):508–509. https://doi.org/10.1038/459508a PMID: 19478766
5. Zhang J, Cunningham JJ, Brown JS, Gatenby RA. Integrating evolutionary dynamics into treatment of metastatic castrate-resistant prostate cancer. Nature Communications. 2017; 8(1):1816. https://doi.org/10.1038/s41467-017-01968-5 PMID: 29180633
6. Kaznatcheev A, Vander Velde R, Scott JG, Basanta D. Cancer treatment scheduling and dynamic heterogeneity in social dilemmas of tumour acidity and vasculature. British journal of cancer. 2017; 116 (6):785–792. https://doi.org/10.1038/bjc.2017.5 PMID: 28183139
7. Bacevic K, Noble R, Soffar A, Wael Ammar O, Boszonyik B, Prieto S, et al. Spatial competition constrains resistance to targeted cancer therapy. Nature communications. 2017; 8(1):1995. https://doi.org/10.1038/s41467-017-01516-1 PMID: 29222471
8. Warman PI, Kaznatcheev A, Araujo A, Lynch CC, Basanta D. Fractionated follow-up chemotherapy delays the onset of resistance in bone metastatic prostate cancer. Games. 2018; 9(2):19. https://doi.org/10.3390/g9020019 PMID: 33552562
9. Yoon N, Vander Velde R, Marusyk A, Scott JG. Optimal therapy scheduling based on a pair of collaterally sensitive drugs. Bulletin of mathematical biology. 2018; 80:1776–1809. https://doi.org/10.1007/s11538-018-0434-2 PMID: 29736596
10. Camacho A, Jerez S. Bone metastasis treatment modeling via optimal control. Journal of mathematical biology. 2019; 78:497–526. https://doi.org/10.1007/s00285-018-1281-3 PMID: 30132065
11. Stanková K, Brown JS, Dalton WS, Gatenby RA. Optimizing Cancer Treatment Using Game Theory: A Review. JAMA Oncology. 2019; 5(1):96. https://doi.org/10.1001/jamaoncol.2018.3395 PMID: 30098166
12. Gluzman M, Scott JG, Vladimirsky A. Optimizing adaptive cancer therapy: dynamic programming and evolutionary game theory. Proceedings of the Royal Society B. 2020; 287(1925):20192454. https://doi.org/10.1098/rspb.2019.2454 PMID: 32315588
13. Yoon N, Krishnan N, Scott J. Theoretical modeling of collaterally sensitive drug cycles: shaping heterogeneity to allow adaptive therapy. Journal of Mathematical Biology. 2021; 83:1–29. https://doi.org/10.1007/s00285-021-01671-6 PMID: 34632539
14. Wölfl B, te Rietmole H, Salvioli M, Kaznatcheev A, Thuijsman F, Brown JS, et al. The contribution of evolutionary game theory to understanding and treating cancer. Dynamic Games and Applications. 2021; p. 1–30. https://doi.org/10.1007/s13235-021-00397-w PMID: 35601872
15. Zhang J, Cunningham J, Brown J, Gatenby R. Evolution-based mathematical models significantly prolong response to abiraterone in metastatic castrate-resistant prostate cancer and identify strategies to further improve outcomes. eLife. 2022; 11:e76284. https://doi.org/10.7554/eLife.76284 PMID: 35762577
16. Hockings H, Lakatos E, Huang W, et al. Adaptive therapy achieves long-term control of chemotherapy resistance in high grade ovarian cancer. Preprint. bioRxiv. 2023;2023.07.21.549688. Published 2023 Jul 25. https://doi.org/10.1101/2023.07.21.549688

17. West J, Adler F, Gallaher J, Strobl M, Brady-Nicholls R, Brown J, et al. A survey of open questions in adaptive therapy: Bridging mathematics and clinical translation. eLife. 2023; 12:e84263. https://doi.org/10.7554/eLife.84263 PMID: 36952376

18. West J, You L, Zhang J, Gatenby RA, Brown JS, Newton PK, et al. Towards Multidrug Adaptive Therapy. Cancer Research. 2020; 80(7):1578–1589. https://doi.org/10.1158/0008-5472.CAN-19-2669 PMID: 31948939

19. Kim E, Brown JS, Eroglu Z, Anderson ARA. Adaptive Therapy for Metastatic Melanoma: Predictions from Patient Calibrated Mathematical Models. Cancers (Basel). 2021 Feb 16; 13(4):823. https://doi.org/10.3390/cancers13040823 PMID: 33669315

20. Gatenby RA, Silva AS, Gillies RJ, Frieden BR. Adaptive Therapy. Cancer Research. 2009; 69 (11):4894–4903. https://doi.org/10.1158/0008-5472.CAN-08-3658 PMID: 19487300

21. Cunningham JJ, Brown JS, Gatenby RA, Staňková K. Optimal control to develop therapeutic strategies for metastatic castrate resistant prostate cancer. Journal of Theoretical Biology. 2018; 459:67–78. https://doi.org/10.1016/j.jtbi.2018.09.022 PMID: 30243754

22. Silva AS, Kam Y, Khin ZP, Minton SE, Gillies RJ, Gatenby RA. Evolutionary Approaches to Prolong Progression-Free Survival in Breast Cancer. Cancer Research. 2012; 72(24):6362–6370. https://doi.org/10.1158/0008-5472.CAN-12-2235 PMID: 23066036

23. Martin RB, Fisher ME, Minchin RF, Teo KL. Optimal control of tumor size used to maximize survival time when cells are resistant to chemotherapy. Mathematical Biosciences. 1992; 110(2):201–219. https://doi.org/10.1016/0025-5564(92)90039-Y PMID: 1498450

24. Monro HC, Gaffney EA. Modelling chemotherapy resistance in palliation and failed cure. Journal of Theoretical Biology. 2009; 257(2):292–302. https://doi.org/10.1016/j.jtbi.2008.12.006 PMID: 19135065

25. Pressley M, Salvioli M, Lewis DB, Richards CL, Brown JS, Staňková K. Evolutionary dynamics of treatment-induced resistance in cancer informs understanding of rapid evolution in natural systems. Frontiers in Ecology and Evolution. 2021; 9:460. https://doi.org/10.3389/fevo.2021.681121

26. Bayer P, Gatenby RA, McDonald PH, Duckett DR, Staňková K, Brown JS. Coordination games in cancer. PLOS ONE. 2022; 17(1):1–15. https://doi.org/10.1371/journal.pone.0261578 PMID: 35061724

27. Stein A, Salvioli M, Garjani H, Dubbeldam J, Viossat Y, Staňková JSBK. Stackelberg Evolutionary Game Theory: How to Manage Evolving Systems. Philosophical Transactions of the Royal Society B. 2023; 378 (1876). https://doi.org/10.1098/rstb.2021.0495 PMID: 36934755

28. Bayer P., West J. Games and the Treatment Convexity of Cancer. Dyn Games Appl 13, 1088–1105 (2023). https://doi.org/10.1007/s13235-023-00520-z

29. Maley CC, Seyedi S, Saha D, Anderson A. Abstract A017: Computational and mouse models of adaptive therapy with multiple drugs in breast cancer. Cancer Res 1 February 2024; 84: A017. https://doi.org/10.1158/1538-7445.CANEVOL23-A017

30. Maltas J, Killarney ST, Singleton KR, et al. Drug dependence in cancer is exploitable by optimally constructed treatment holidays. Nat Ecol Evol 8, 147–162 (2024). https://doi.org/10.1038/s41559-023-02255-x PMID: 38012363

31. Viossat Y, Noble R. A theoretical analysis of tumour containment. Nature Ecology & Evolution. 2021; 5 (6):826–835. https://doi.org/10.1038/s41559-021-01428-w PMID: 33846605

32. Staňková K. Resistance games. Nature Ecology & Evolution. 2019; 3(3):336–337. https://doi.org/10.1038/s41559-018-0785-y PMID: 30778182

33. Kam Y, Das T, Tian H, Foroutan P, Ruiz E, Martinez G, et al. Sweat but no gain: Inhibiting proliferation of multidrug resistant cancer cells with "ersatzdroges": Inhibiting MDR cancer cells with ersatzdroges. International Journal of Cancer. 2015; 136(4):E188–E196. https://doi.org/10.1002/ijc.29158 PMID: 25156304

34. Kaznatcheev A, Peacock J, Basanta D, Marusyk A, Scott JG. Fibroblasts and alectinib switch the evolutionary games played by non-small cell lung cancer. Nature Ecology & Evolution. 2019; 3(3):450–456. https://doi.org/10.1038/s41559-018-0768-z PMID: 30778184

35. Strobl MAR, West J, Viossat Y, Damaghi M, Robertson-Tessi M, Brown JS, et al. Turnover Modulates the Need for a Cost of Resistance in Adaptive Therapy. Therapy Cancer Res. 2021; 81(4):1135–1147. https://doi.org/10.1158/0008-5472.CAN-20-0806 PMID: 33172930

36. Brady R, Enderling H. Mathematical Models of Cancer: When to Predict Novel Therapies, and When Not to. Bulletin of Mathematical Biology. 2019; 81(10):3722–3731. https://doi.org/10.1007/s11538-019-00640-x PMID: 31338741

37. Lee ND, Kaveh K, Bozic I. Clonal interactions in cancer: integrating quantitative models with experimental and clinical data. In: Seminars in Cancer Biology. vol. 92. Elsevier; 2023. p. 61–73.

38. Ghaffari Laleh N, Loeffler CML, Grajek J, Staňková K, Pearson AT, Muti HS, et al. Classical mathematical models for prediction of response to chemotherapy and immunotherapy. PLOS Computational Biology. 2022; 18(2):e1009822. https://doi.org/10.1371/journal.pcbi.1009822 PMID: 35120124

39. Spigel DR, Chaft JE, Gettinger S, Chao BH, Dirix L, Schmid P, et al. FIR: Efficacy, Safety, and Biomarker Analysis of a Phase II Open-Label Study of Atezolizumab in PD-L1–Selected Patients With NSCLC. Journal of Thoracic Oncology. 2018; 13(11):1733–1742. https://doi.org/10.1016/j.jtho.2018.05.004 PMID: 29775807

40. Fehrenbacher L, Spira A, Ballinger M, Kowanetz M, Vansteenkiste J, Mazieres J, et al. Atezolizumab versus docetaxel for patients with previously treated non-small-cell lung cancer (POPLAR): a multicentre, open-label, phase 2 randomised controlled trial. The Lancet. 2016; 387(10030):1837–1846. https://doi.org/10.1016/S0140-6736(16)00587-0

41. Peters S, Gettinger S, Johnson ML, Jänne PA, Garassino MC, Christoph D, et al. Phase II Trial of Atezolizumab As First-Line or Subsequent Therapy for Patients With Programmed Death-Ligand 1—Selected Advanced Non–Small-Cell Lung Cancer (BIRCH). Journal of Clinical Oncology. 2017; 35(24):2781–2789. https://doi.org/10.1200/JCO.2016.71.9476 PMID: 28609226

42. Rittmeyer A, Barlesi F, Waterkamp D, Park K, Ciardiello F, von Pawel J, et al. Atezolizumab versus docetaxel in patients with previously treated non-small-cell lung cancer (OAK): a phase 3, open-label, multicentre randomised controlled trial. The Lancet. 2017; 389(10066):255–265. https://doi.org/10.1016/S0140-6736(16)32517-X

43. Beal L, Hill D, Martin R, Hedengren J. GEKKO Optimization Suite. Processes. 2018; 6(8):106. https://doi.org/10.3390/pr6080106

44. Sahai E, Astsaturov I, Cukierman E, DeNardo DG, Egeblad M, Evans RM, et al. A framework for advancing our understanding of cancer-associated fibroblasts. Nature Reviews Cancer. 2020; 20(3):174–186. https://doi.org/10.1038/s41568-019-0238-1 PMID: 31980749

45. Faustino-Rocha A, Oliveira PA, Pinho-Oliveira J, Teixeira-Guedes C, Soares-Maia R, da Costa RG, et al. Estimation of rat mammary tumor volume using caliper and ultrasonography measurements. Lab Animal. 2013; 42(6):217–224. https://doi.org/10.1038/laban.254 PMID: 23689461

46. Kaznatcheev A, Lin CH. Measuring as a new mode of inquiry that bridges evolutionary game theory and cancer biology. Philosophy of Science. 2022; 89(5):1124–1133. https://doi.org/10.1017/psa.2022.57

47. Archetti M, Ferraro DA, Christofori G. Heterogeneity for IGF-II production maintained by public goods dynamics in neuroendocrine pancreatic cancer. Proceedings of the National Academy of Sciences. 2015; 112(6):1833–1838. https://doi.org/10.1073/pnas.1414653112 PMID: 25624490

48. Bhattacharya R, Vander Velde R, Marusyk V, Desai B, Kaznatcheev A, Marusyk A, et al. Understanding the evolutionary games in NSCLC microenvironment. bioRxiv. 2020; p. 2020–11. https://doi.org/10.1101/2020.11.30.404350

49. Noble RJ, Walther V, Roumestand C, Hochberg ME, Hibner U, Lassus P. Paracrine behaviors arbitrate parasite-like interactions between tumor subclones. Frontiers in ecology and evolution. 2021; 9:675638. https://doi.org/10.3389/fevo.2021.675638 PMID: 35096847

50. Farrokhian N, Maltas J, Dinh M, Durmaz A, Ellsworth P, Hitomi M, et al. Measuring competitive exclusion in non–small cell lung cancer. Science Advances. 2022; 8(26):eabm7212. https://doi.org/10.1126/sciadv.abm7212 PMID: 35776787

51. Cho H, Lewis AL, Storey KM, Byrne HM. Designing experimental conditions to use the Lotka–Volterra model to infer tumor cell line interaction types. Journal of Theoretical Biology. 2023; 559:111377. https://doi.org/10.1016/j.jtbi.2022.111377 PMID: 36470468

52. Strobl M, Martin A, West J, Gallaher J, Robertson-Tessi M, Gatenby R, et al. Adaptive therapy for ovarian cancer: An integrated approach to PARP inhibitor scheduling. bioRxiv. 2023; p. 2023–03. https://doi.org/10.1101/2023.03.22.533721

53. Enriquez-Navas PM, Wojtkowiak JW, Gatenby RA. Application of Evolutionary Principles to Cancer Therapy. Cancer Research. 2015; 75(22):4675–4680. https://doi.org/10.1158/0008-5472.CAN-15-1337 PMID: 26527288